Supplement of Evaluation of the University of Victoria Earth system climate model version 2.10 (UVic ESCM 2.10)

Nadine Mengis[1,2], David P. Keller[1], Andrew MacDougall[3], Michael Eby[4], Nesha Wright[2], Katrin J. Meissner[5], Andreas Oschlies[1], Andreas Schmittner[6], H. Damon Matthews[7], Kirsten Zickfeld[2]

[1]Biogeochemical Modelling Department, GEOMAR – Helmholtz Centre for Ocean Research, Kiel, Germany
[2]Geography Department, Simon Fraser University, Burnaby, BC, Canada
[3]Climate and Environment, St. Francis Xavier University, Antigonish, NS, Canada
[4]School of Earth and Ocean Sciences, University of Victoria, Victoria, BC, Canada
[5]Climate Change Research Centre, The University of New South Wales, Sydney, New South Wales, Australia and The Australian Research Council Centre of Excellence for Climate Extremes, Sydney, New South Wales, Australia
[6]College of Earth, Ocean, and Atmospheric Sciences, Oregon State University, Corvallis, OR, USA
[7]Concordia University, Montréal, Canada

Correspondence to: Nadine Mengis (nmengis@geomar.de)

Abstract. The University of Victoria Earth system climate model of intermediate complexity has been a useful tool in recent assessments of long-term climate changes including paleo-climate modelling. Since the last official release of the UVic ESCM 2.9, and the two official updates during the last decade, a lot of model development has taken place in multiple groups. The new version 2.10 of the University of Victoria Earth System Climate Model (UVic ESCM), to be used in the 6th phase of the coupled model intercomparison project (CMIP6), presented here combines and brings together multiple model developments and new components that have taken place since the last official release of the model. To set the foundation of its use, we here describe the UVic ESCM 2.10 and evaluate results from transient historical simulations against observational data. We find that the UVic ESCM 2.10 is capable of reproducing well changes in historical temperature and carbon fluxes, as well as the spatial distribution of many ocean tracers, like temperature, salinity, phosphate and nitrate. This is connected to a good representation of ocean physical properties. For the moment, there remain biases in ocean alkalinity and dissolved inorganic carbon, which will be addressed in the next updates to the model.

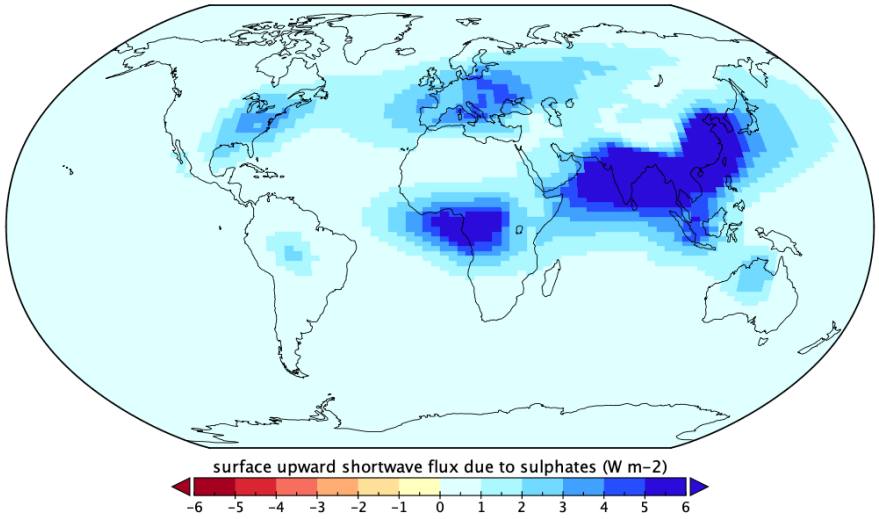

Figure S1: Clear-sky effective radiative forcing (ERF) from sulphate aerosols in the UVic ESCM 2.10. The global mean ERF amounts to 0.99 W m^{-2}, for comparison Stevens et al., 2017 have a global mean clear sky ERF of 0.67 W m^{-2}.

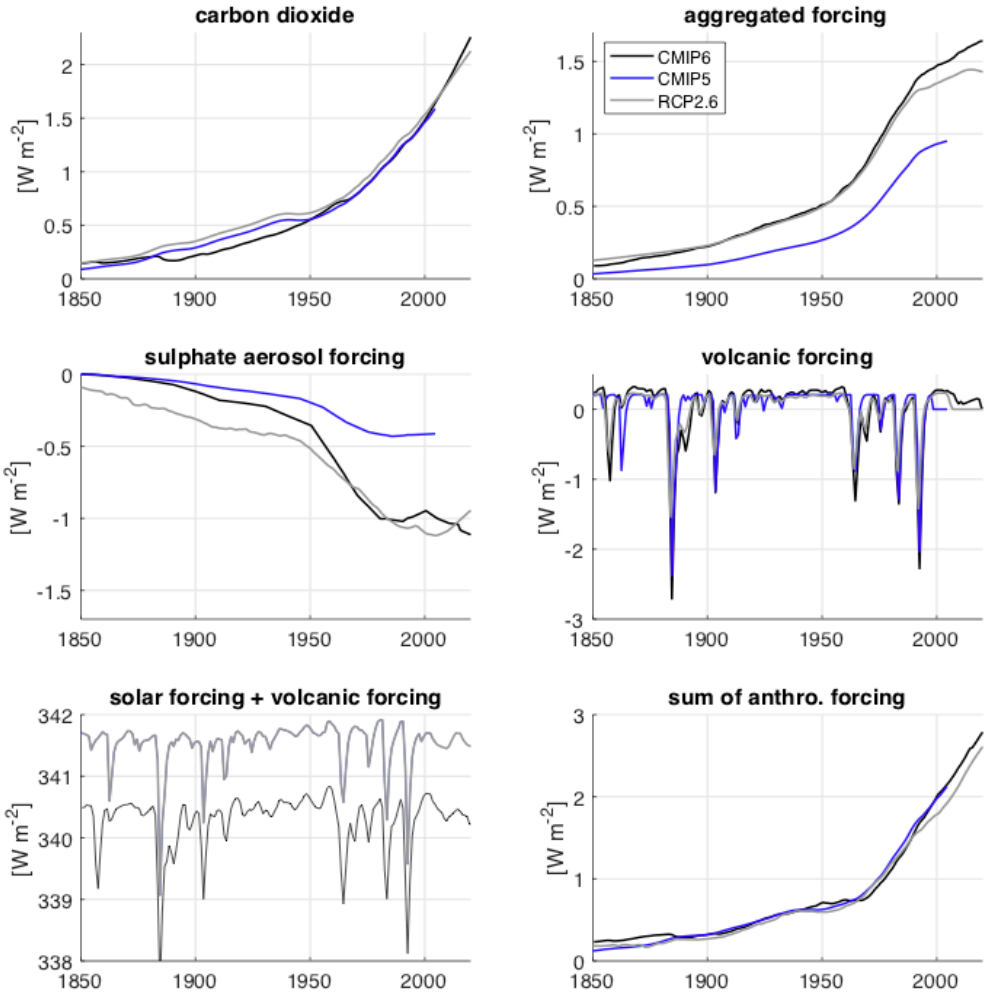

Figure S2: Comparison of radiative forcing used for the UVic ESCM for the Coupled Model Intercomparison Projects 5 and 6 (CMIP5 and CMIP6, respectively) and the data for the historical period as given by IMAGE model (Meinshausen et al., 2011). Detailed description see section 2.2 of the main article.

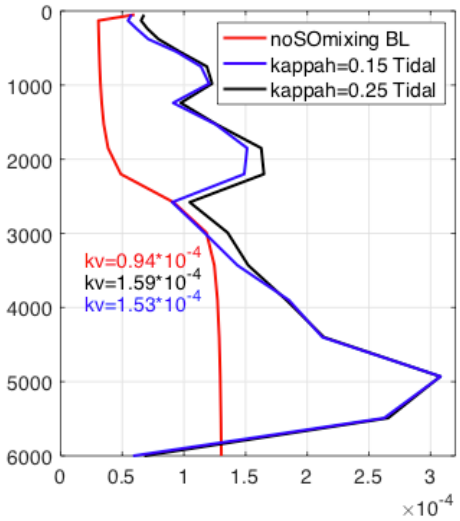

Figure S3: Vertical profiles of diffusivity in units of $m^2\ s^{-1}$ for the model version UVic ESCM 2.9 as published by Eby et al., 2013 with the Bryan-Lewis vertical mixing scheme and no increased mixing in the Southern Ocean (noSOmixing BL), the UVic ESCM 2.9 as published by Keller et al., 2013 with a tidal mixing scheme increased Southern Ocean mixing and a background diffusivity of 0.15 (kappah=0.15 Tidal), and finally the UVic ESCM 2.10 with the same mixing scheme as Keller et al., 2013 but increased background diffusivity of 0.25 (kappah=0.15 Tidal).

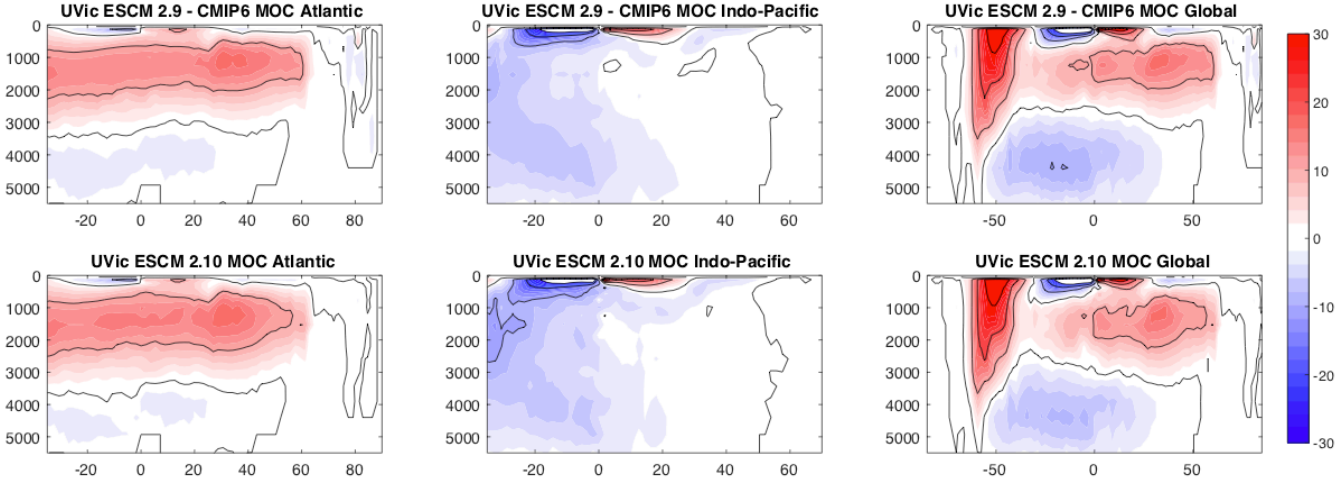

Figure S4: Ocean section of meridional overturning in units of Sv for the Atlantic Ocean including the Arctic Ocean (left column), the Indo-Pacific Ocean (middle column), and the global average (left column). From top to bottom are shown the published UVic ESCM version 2.9 by (Eby et al., 2013) spun-up and forced with CMIP6 forcing, and the UVic ESCM version 2.10, both as a mean of the 1980-2010 period.

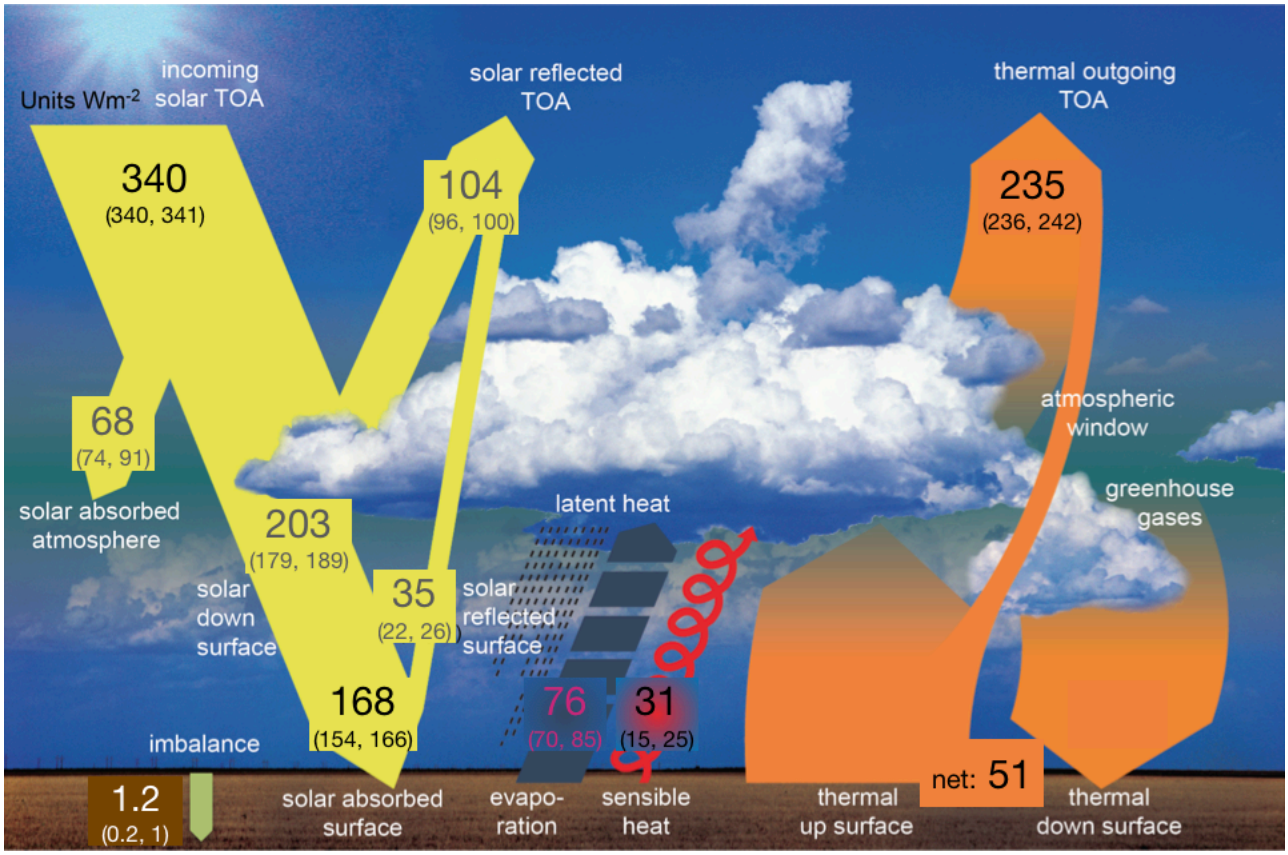

Figure S5: Schematic diagram of the global mean energy balance of the UVic ESCM 2.10. Magnitudes of the globally averaged energy balance components, black numbers indicate estimates directly taken from the model output, grey numbers have been derived by calculations given albedo values from the model, and the latent heat was calculated using the evaporation estimates from the model assuming a conversion factor of 2,260 kJ/kg. Uncertainty ranges are taken from (Wild et al., 2013), representing present day climate conditions at the beginning of the 21th century. Units Wm-2.

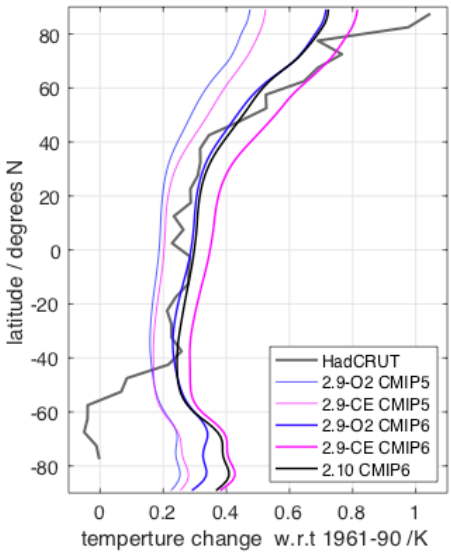

Figure S6: Zonal means of temperature change of the HadCRUT median near surface temperature anomaly (grey line) (Morice et al., 2012) in comparison to the model version UVic ESCM 2.9 as published by Eby et al., 2013 (2.9-02 CMIP5), the UVic ESCM 2.9 as published by Keller et al., 2013 (2.9-CE CMIP5), these models spun-up and forced with CMIP6 protocol, and the UVic ESCM 2.10. All temperature changes are for a 30-years mean around 1995 with respect to the 1961-1990 period in K.

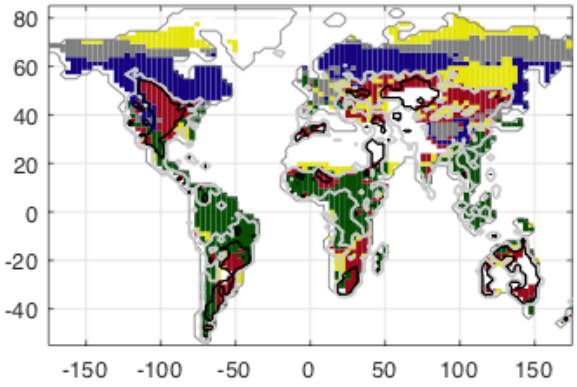

Figure S7: Map of predominant plant functional types in the UVic ESCM 2.10 for the period of 1980-2010, color indicate broadleaf tree (green), needleleaf tree (blue), C3 and C4 grasses (yellow), crops (red) and shrubs (grey).

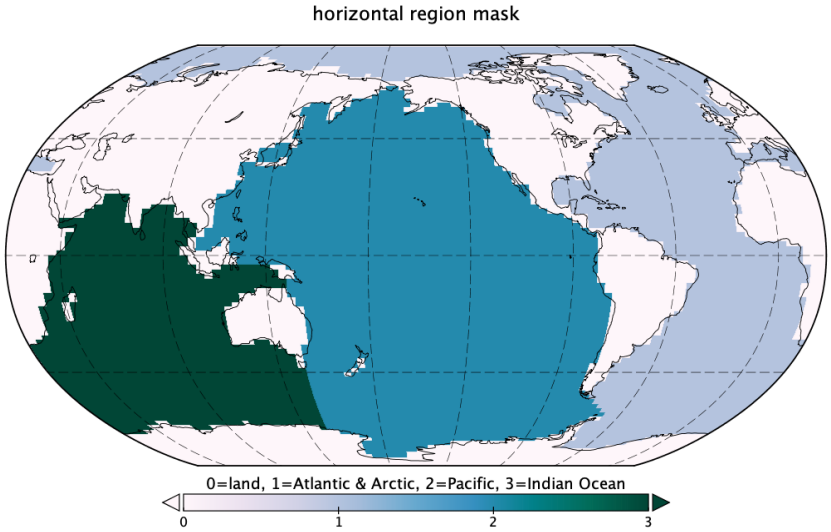

Figure S8: Map showing the partitioning of the UVic ESCM into different ocean basins.

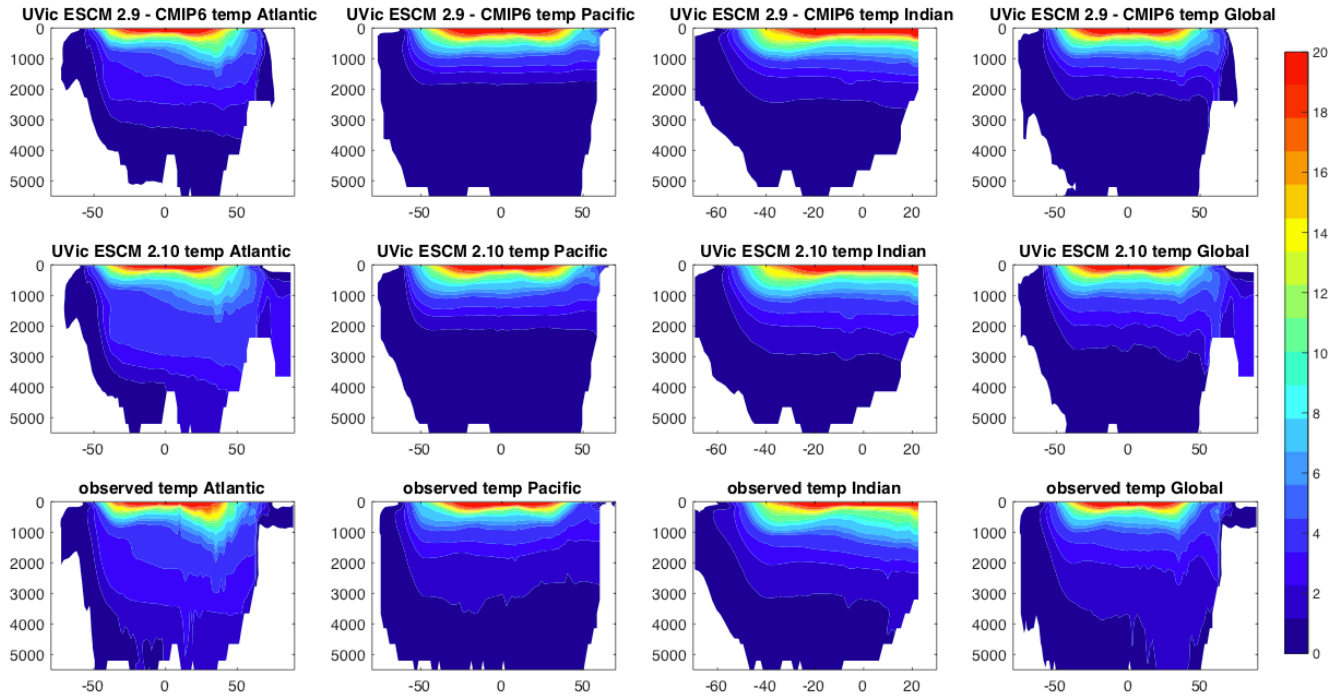

Figure S9: Ocean section of temperature in units of °C for the Atlantic Ocean including the Arctic Ocean (left column), the Pacific Ocean (middle left column), the Indian Ocean (middle right column) and the global average (left column) compared to World Ocean Atlas 2018 (Locarnini et al., 2019). From top to bottom are shown the published UVic ESCM version 2.9 by (Eby et al., 2013) spun-up and forced with CMIP6 forcing, the UVic ESCM version 2.10, both as a mean of the periods 1980-2010 and the observed ocean sections.

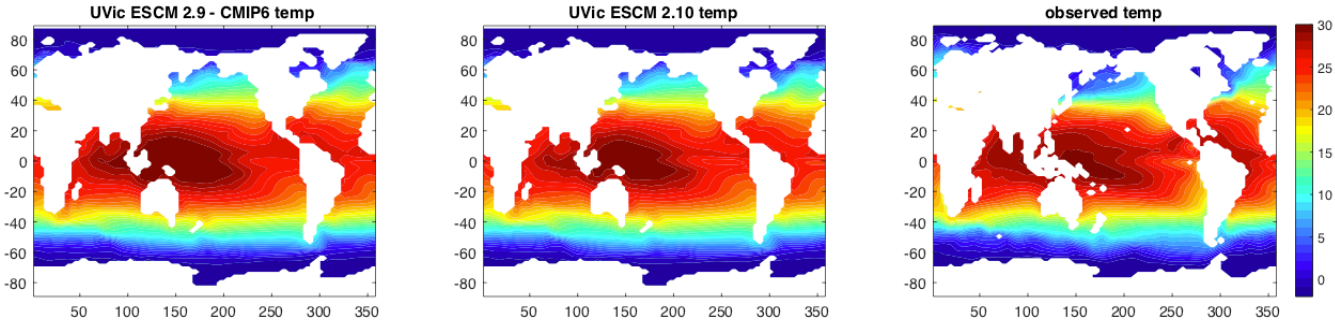

Figure S10: Maps of sea surface temperature in units of °C for the published UVic ESCM version 2.9 (Eby et al., 2013) spun-up and forced with CMIP6 forcing, for the UVic ESCM 2.10, and for the World Ocean Atlas 2018 (Locarnini et al., 2019).

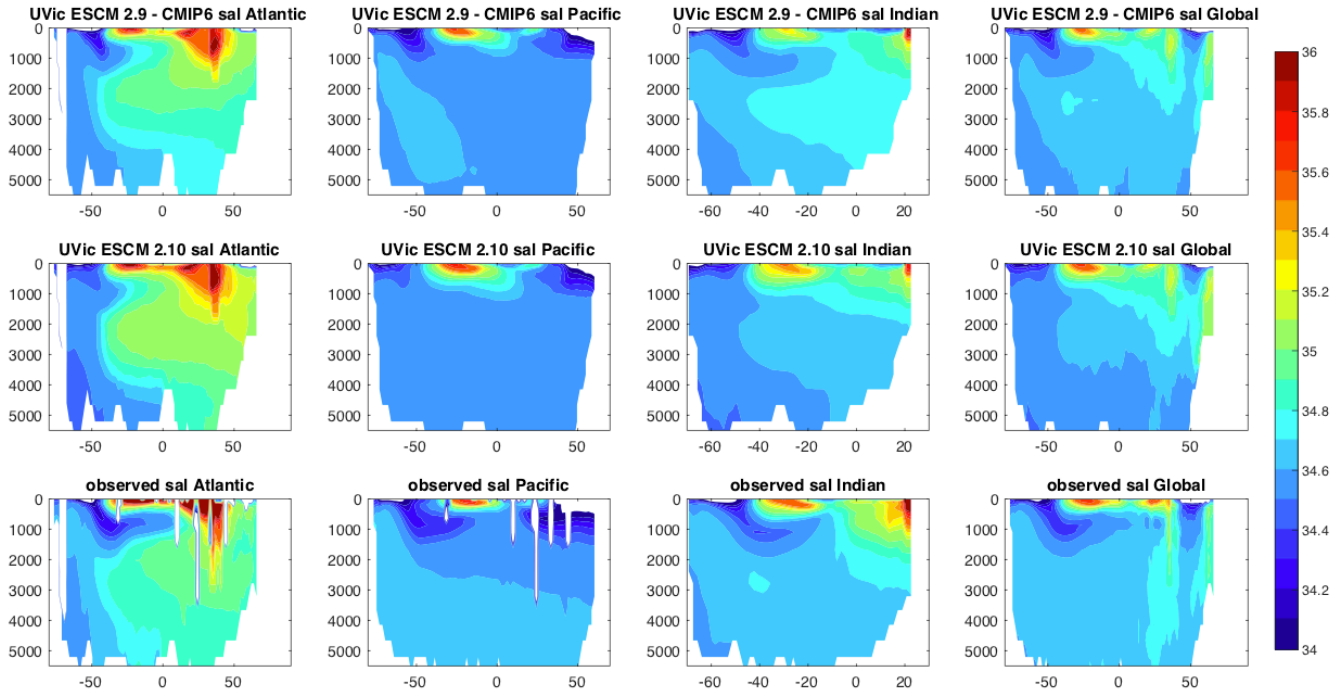

Figure S11: Ocean section of salinity in units of psu for the Atlantic Ocean including the Arctic Ocean (left column), the Pacific Ocean (middle left column), the Indian Ocean (middle right column) and the global average (left column) compared to World Ocean Atlas 2018 (Locarnini et al., 2019). From top to bottom are shown the published UVic ESCM version 2.9 by (Eby et al., 2013) spun-up and forced with CMIP6 forcing, the UVic ESCM version 2.10, both as a mean of the periods 1980-2010 and the observed ocean sections.

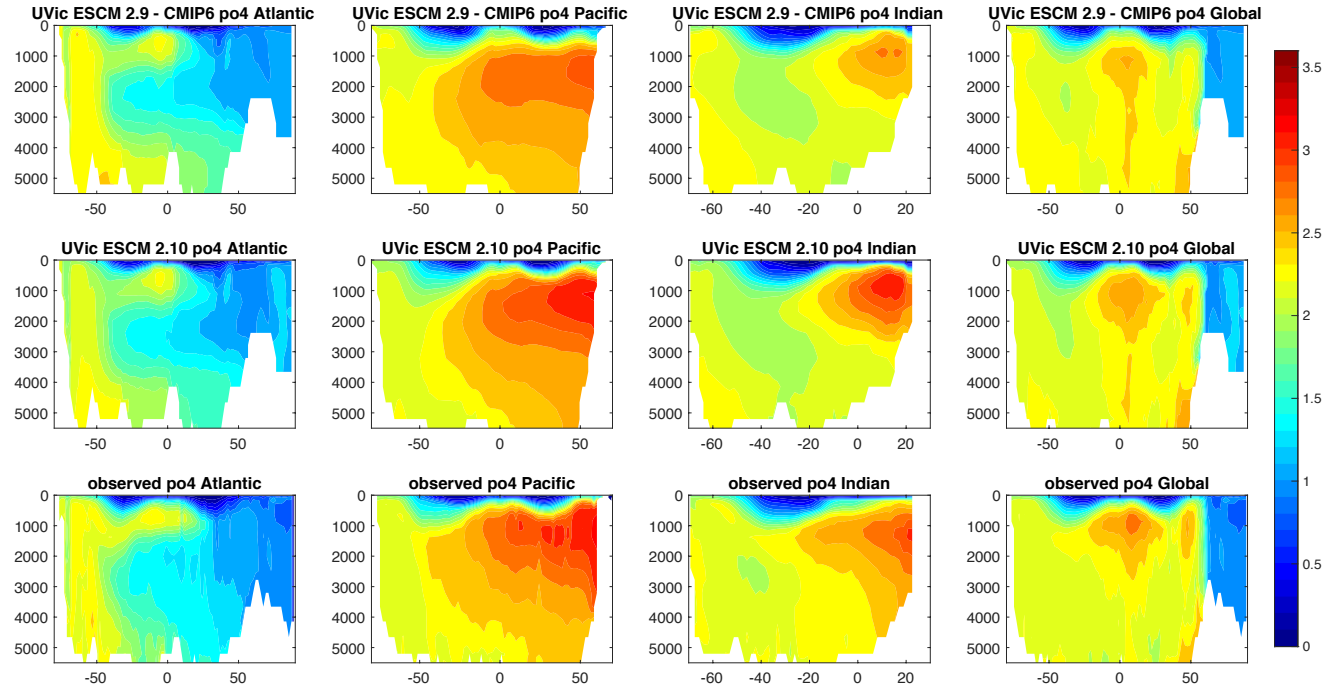

Figure S12: Ocean section of PO_4 in units of µmol kg^{-1} for the Atlantic Ocean including the Arctic Ocean (left column), the Pacific Ocean (middle left column), the Indian Ocean (middle right column) and the global average (left column) compared to World Ocean Atlas 2018 (Garcia et al., 2019). From top to bottom are shown the published UVic ESCM version 2.9 by (Eby et al., 2013) spun-up and forced with CMIP6 forcing, the UVic ESCM version 2.10, both as a mean of the periods 1980-2010 and the observed ocean sections.

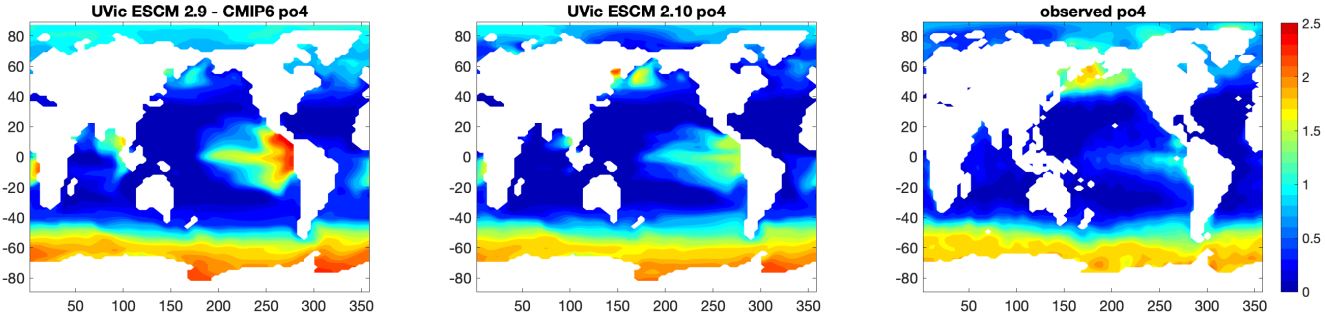

Figure S13: Maps of sea surface PO_4 in units of µmol kg^{-1} for the published UVic ESCM version 2.9-02 (Eby et al., 2013) spun-up and forced with CMIP6 forcing, for the UVic ESCM 2.10, and for the World Ocean Atlas 2018 (Garcia et al., 2019).

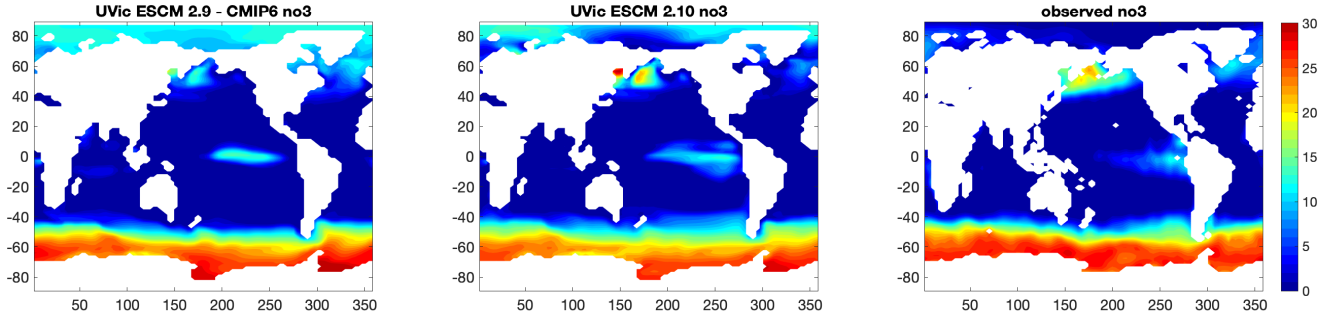

Figure S14: Maps of sea surface NO_3 in units of µmol kg^{-1} for the published UVic ESCM version 2.9-02 (Eby et al., 2013) spun-up and forced with CMIP6 forcing, for the UVic ESCM 2.10, and for the World Ocean Atlas 2018 (Garcia et al., 2019).

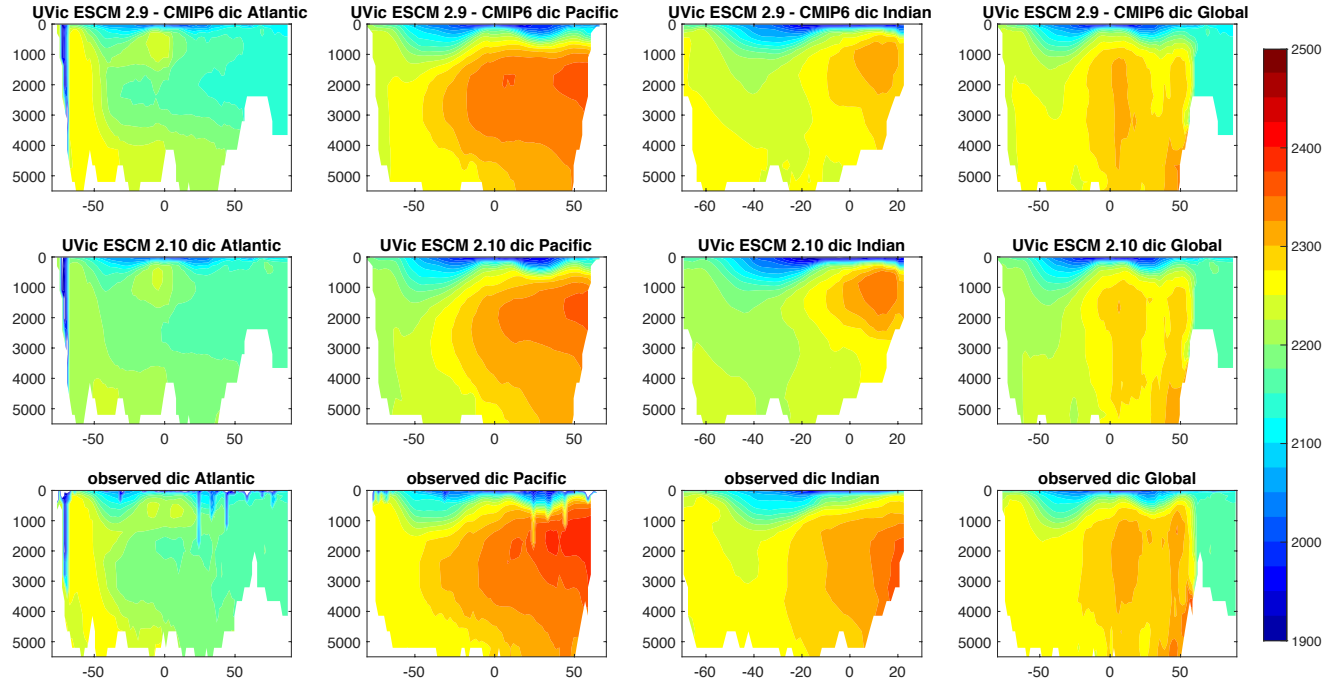

Figure S15: Ocean section of dissolved inorganic carbon in units of µmol kg^{-1} for the Atlantic Ocean including the Arctic Ocean (left column), the Pacific Ocean (middle left column), the Indian Ocean (middle right column) and the global average (left column) compared to Global Ocean Data Analysis Project (GLODAP) mapped climatologies version 2 (Lauvset et al., 2016). From top to bottom are shown the published UVic ESCM version 2.9 by (Eby et al., 2013) spun-up and forced with CMIP6 forcing, the UVic ESCM version 2.10, both as a mean of the periods 1980-2010 and the observed ocean sections.

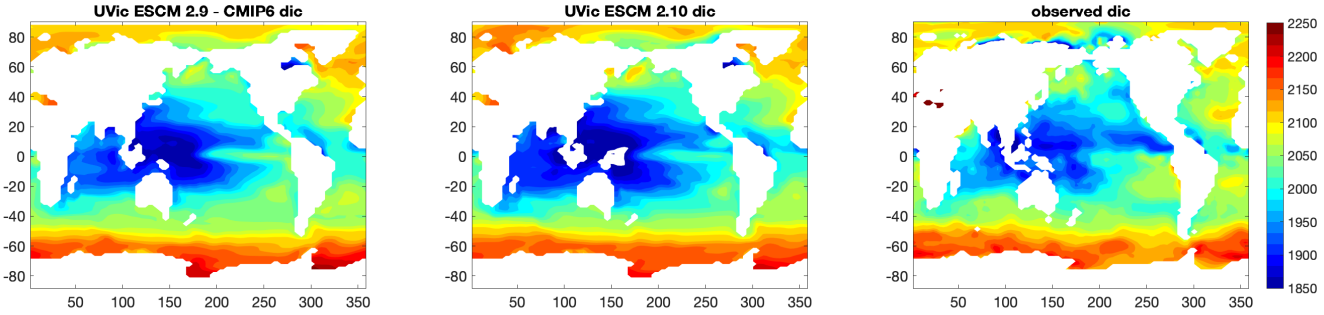

Figure S16: Maps of sea surface dissolved inorganic carbon in units of µmol kg^{-1} for the published UVic ESCM version 2.9-02 (Eby et al., 2013) spun-up and forced with CMIP6 forcing, for the UVic ESCM 2.10, and for the Global Ocean Data Analysis Project (GLODAP) mapped climatologies version 2 (Lauvset et al., 2016).

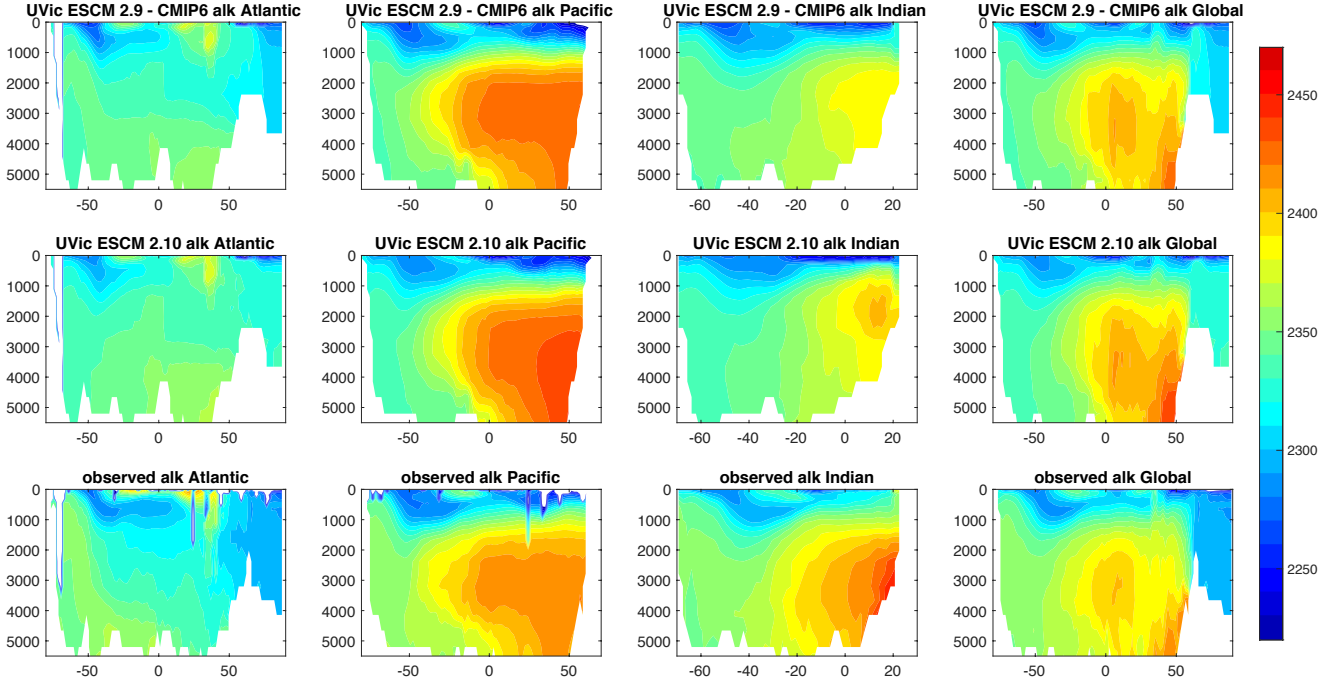

Figure S17: Ocean section of alkalinity in units of µmol kg^{-1} for the Atlantic Ocean including the Arctic Ocean (left column), the Pacific Ocean (middle left column), the Indian Ocean (middle right column) and the global average (left column) compared to Global Ocean Data Analysis Project (GLODAP) mapped climatologies version 2 (Lauvset et al., 2016). From top to bottom are shown the published UVic ESCM version 2.9 by (Eby et al., 2013) spun-up and forced with CMIP6 forcing, the UVic ESCM version 2.10, both as a mean of the periods 1980-2010 and the observed ocean sections.

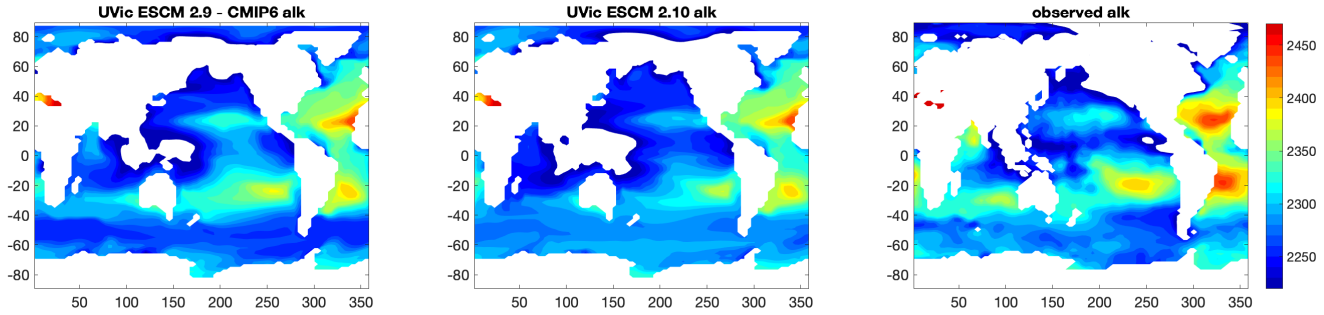

Figure S18: Maps of sea surface alkalinity in units of µmol kg^{-1} for the published UVic ESCM version 2.9-02 (Eby et al., 2013) spun-up and forced with CMIP6 forcing, for the UVic ESCM 2.10, and for the Global Ocean Data Analysis Project (GLODAP) mapped climatologies version 2 (Lauvset et al., 2016).

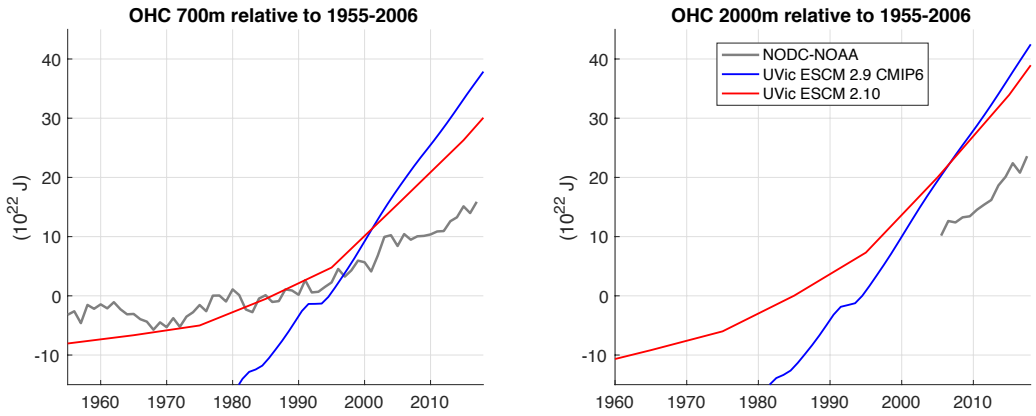

Figure S19: Time series of ocean heat content (OHC) anomalies with respect to the 1955 to 2006 period of the UVic ESCM 2.10 (red line) in comparison with observations from (Levitus et al., 2012).

References

Eby, M., Weaver, A. J., Alexander, K., Zickfeld, K., Abe-Ouchi, A., Cimatoribus, A. A., Crespin, E., Drijfhout, S. S., Edwards, N. R., Eliseev, A. V., Feulner, G., Fichefet, T., Forest, C. E., Goosse, H., Holden, P. B., Joos, F., Kawamiya, M., Kicklighter, D., Kienert, H., Matsumoto, K., Mokhov, I. I., Monier, E., Olsen, S. M., Pedersen, J. O. P., Perrette, M., Philippon-Berthier, G., Ridgwell, A., Schlosser, A., Von Deimling, T. S., Shaffer, G., Smith, R. S., Spahni, R., Sokolov, A. P., Steinacher, M., Tachiiri, K., Tokos, K., Yoshimori, M., Zeng, N. and Zhao, F.: Historical and idealized climate model experiments: An intercomparison of Earth system models of intermediate complexity, Clim. Past, 9(3), 1111–1140, doi:10.5194/cp-9-1111-2013, 2013.

Garcia, H. E., Weathers, K. W., Paver, C. R., Smolyar, I., Boyer, T. P., Locarnini, R. A., Zweng, M. M., Mishonov, A. V., Baranova, O. K., Seidov, D. and Reagan, J. R.: WORLD OCEAN ATLAS 2018 Volume 3: Dissolved Oxygen, Apparent Oxygen Utilization, and Dissolved Oxygen Saturation, NOAA Atlas NESDIS 83, 1(September), 38pp, 2019a.

Garcia, H. E., Weathers, K. W., Paver, C. R., Smolyar, I., Boyer, T. P., Locarnini, R. A., Zweng, M. M., Mishonov, A. V., Baranova, O. K., Seidov, D. and Reagan, J. R.: WORLD OCEAN ATLAS 2018 Volume 4: Dissolved Inorganic Nutrients (phosphate, nitrate and nitrate+nitrite, silicate), NOAA Atlas NESDIS 84, 2019b.

Lauvset, S. K., Key, R. M., Olsen, A., Van Heuven, S., Velo, A., Lin, X., Schirnick, C., Kozyr, A., Tanhua, T., Hoppema, M., Jutterström, S., Steinfeldt, R., Jeansson, E., Ishii, M., Perez, F. F., Suzuki, T. and Watelet, S.: A new global interior ocean mapped climatology:

Levitus, S., Antonov, J. I., Boyer, T. P., Baranova, O. K., Garcia, H. E., Locarnini, R. A., Mishonov, A. V., Reagan, J. R., Seidov, D., Yarosh, E. S. and Zweng, M. M.: World ocean heat content and thermosteric sea level change (0-2000m), 1955-2010, Geophys. Res. Lett., 39(10), 1–5, doi:10.1029/2012GL051106, 2012.

Locarnini, R. A., Mishonov, A. V., Baranova, O. K., Boyer, T. P., Zweng, M. M., Garcia, H. E., Reagan, J. R., Seidov, D., Weathers, K. W., Paver, C. R. and Smolyar, I. V.: World Ocean Atlas, Volume 1: Temperature, , 1(July), 52 [online] Available from: http://www.nodc.noaa.gov/OC5/indprod.html, 2019.

Meinshausen, M., Smith, S. J., Calvin, K. V., Daniel, J. S., Kainuma, M. L. T., Lamarque, J., Matsumoto, K., Montzka, S. A., Raper, S. C. B., Riahi, K., Thomson, A. M., Velders, G. J. M. and van Vuuren, D. P.: The RCP greenhouse gas concentrations and their extensions from 1765 to 2300, Clim. Change, 109(1), 213–241, doi:10.1007/s10584-011-0156-z, 2011.

Morice, C. P., Kennedy, J. J., Rayner, N. A. and Jones, P. D.: Quantifying uncertainties in global and regional temperature change using an ensemble of observational estimates: The HadCRUT4 data set, J. Geophys. Res. Atmos., 117(D8), 2012.

Wild, M., Folini, D., Schär, C., Loeb, N., Dutton, E. G. and König-Langlo, G.: The global energy balance from a surface perspective, Clim. Dyn., 40(11–12), 3107–3134, doi:10.1007/s00382-012-1569-8, 2013.

Zweng, M. ., Reagan, J. R., Seidov, D., Boyer, T. P., Locarnini, R. A., Garcia, H. E., Mishonov, A. V., Baranova, O. K., Weathers, K. W., Paver, C. R. and Smolyar, I. V.: World Ocean Atlas 2018, Volume 2: Salinity, , 2(September), 2019.